Chinese Chemical Letters 37 (2026) 111410

Contents lists available at ScienceDirect

Chinese Chemical Letters

journal homepage: www.elsevier.com/locate/cclet

Vaccination of STING agonists-loaded nanoemulsions for cancer immunotherapy

Xue Ma[a,1], Anning Li[b,1], Zhiliang Gao[c], Ning Wang[a], Mengqi Li[a], Kanaparedu P.C. Sekhar[a], Muthupandian Ashokkumar[d], Shumei Zhai[a], Jiwei Cui[a], Qun Yu[a,*]

[a] Key Laboratory of Colloid and Interface Chemistry of the Ministry of Education, School of Chemistry and Chemical Engineering, Shandong University, Ji'nan 250100, China
[b] Department of Radiology, Qilu Hospital, Cheeloo College of Medicine, Shandong University, Ji'nan 250012, China
[c] Shandong Key Laboratory of Magnetic Field-free Medicine & Functional Imaging, Research Institute of Magnetic Field-free Medicine & Functional Imaging, National Medicine-Engineering Interdisciplinary Industry-Education Integration Innovation Platform, Shandong University, Ji'nan 250012, China
[d] School of Chemistry, The University of Melbourne, Parkville, VIC 3010, Australia

ARTICLE INFO

Article history:
Received 4 March 2025
Revised 3 June 2025
Accepted 5 June 2025
Available online 6 June 2025

Keywords:
Cancer vaccine
Adjuvants
STING agonists
Nanoemulsion
Immunotherapy

ABSTRACT

Cancer vaccines have proven to be a powerful tool in anti-tumor immunotherapy, leveraging antigen-specific T-cell responses. The effective activation of the stimulator of the interferon gene (STING) protein signal pathway by natural or synthetic agonists leads to the creation of a pro-immune tumor microenvironment. Here, we report the preparation of ovalbumin (OVA) loaded cancer vaccines based on nanoemulsions, denoted as DMMF59-OVA, for the co-delivery of antigens and a STING agonist (MSA-2). The nanovaccines were obtained *via* encapsulation of MSA-2 into squalene phase, which was stabilized by surfactants and coated with OVA. Upon intramuscular administration, the engineered nanovaccine facilitates antigen internalization, maturation of antigen-presenting cells (APCs), and efficient activation of the STING pathway. These results in enhanced antigen-specific humoral and cellular immune responses that significantly inhibit tumor growth in an E.G7-OVA mouse model. The studies provide an avenue for the application of nanovaccine in tumor immunotherapy. Given the ease of preparation and tunable physicochemical properties, DMMF59-OVA represents a promising therapeutic nanovaccine for biomedical applications

© 2026 Published by Elsevier B.V. on behalf of Chinese Chemical Society and Institute of Materia Medica, Chinese Academy of Medical Sciences.

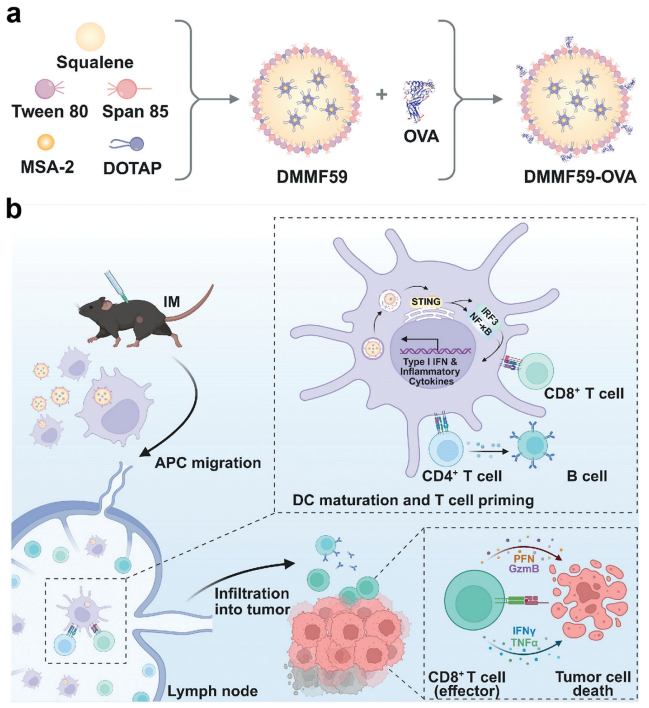
Immunotherapy utilizing the innate and adaptive immune systems to fight against tumor cells has dramatically revolutionized cancer treatment [1]. Cancer vaccines, chimeric antigen receptor-T (CAR-T) cells, and immune checkpoint inhibitors represent advancements in tumor immunotherapy [2–6]. However, challenges such as low immunogenicity, unreliable response rates and tumor-intrinsic resistance to immunity have limited their clinical efficacy of therapeutic options for tumors [7–10]. In context of vaccine development, adjuvants are crucial for enhancing the magnitude and durability of the immune response, thereby bolstering the effectiveness and longevity of vaccines [11–13].

Stimulator of interferon genes (STING) is a membrane-bound protein found in the endoplasmic reticulum, which can be activated by the molecule 2′,3′-cyclic guanosine monophosphate–adenosine monophosphate (cGAMP). This molecule is generated by cGAMP synthase (cGAS), a DNA sensor located in the cytoplasm [14–17]. STING pathway activation, accompanied by interferon-β (IFN-β) secretion, enhances antitumor immunity [18–23]. This process boosts dendritic cell (DC) maturation, antigen presentation, effector T cell proliferation, and thereby augments immunotherapy efficacy [24–27]. STING agonists such as cyclic dinucleotides (CDNs), small-molecule synthetic drugs and metal ions (Mn^{2+}, Zn^{2+}) have shown encouraging therapeutic potential [16,28–30]. MSA-2, a non-nucleotide STING agonist with well metabolic stability for systemic administration, can directly bind to STING, triggering downstream signaling and pro-inflammatory cytokine/interferon (tumor necrosis factors (TNFs), interleukin-6 (IL-6), IFN-β) production [31–36]. However, the poor water solubility and off-target distribution hinder their translation into practical applications [37]. Developing a novel nanocarrier is imperative to enhance STING agonists' pharmacological activity and promote their integration into tumor vaccines.

In addition to endogenous or synthesized small molecules, emulsion-based adjuvants can recruit and activate antigen-

* Corresponding author.
E-mail address: qunyu@sdu.edu.cn (Q. Yu).
[1] These authors contributed equally to this work.

https://doi.org/10.1016/j.cclet.2025.111410
1001-8417/© 2026 Published by Elsevier B.V. on behalf of Chinese Chemical Society and Institute of Materia Medica, Chinese Academy of Medical Sciences.



Scheme 1. (a) Preparation of nanoemulsion-based delivery system loaded with OVA and MSA-2. (b) After intramuscular injection (IM), DMMF59-OVA efficiently accumulated in lymph nodes, induced DC maturation and antigen cross-presentation, activated antigen-specific humoral and cellular immune responses to eliminate tumor cells.

presenting cells (APCs), inducing antigen-specific adaptive immune responses [38–42]. MF59, an emulsion-based adjuvant approved by the Food and Drug Administration (FDA), has demonstrated its potential during past pandemic influenza outbreaks with good biosafety, antigen-sparing effects, and enhanced immunogenicity [43–45]. Nevertheless, neither of these can elicit an effective cell-mediated immune response, which is crucial in the development of vaccines for the treatment of cancers and specific infectious diseases [46]. Moreover, their weak interaction with antigen molecules limits their immune efficacy as antigen delivery carriers [47,48].

In this study, we prepared a nanoemulsion-based vaccine delivery system by incorporating a cationic lipid (2,3-dioleyl-propyl)-trimethylamine (DOTAP) into the existing MF59 emulsion for the encapsulation of MSA-2 and ovalbumin (OVA), where the vaccine was denoted as DMMF59-OVA (Scheme 1). Consequently, it facilitated the cellular internalization of OVA and MSA-2, activation of the STING pathway, and the enhanced humoral and cellular immune responses, leading to the inhibition of E.G7-OVA tumor growth. This study highlights the potential of the emulsion-based nanovaccines for improved antitumor immunity.

Before the emulsification process, MSA-2, DOTAP and squalene were dissolved in chloroform. Subsequently, the oil phase was broken up into smaller droplets under the continuous ultrasonic shearing (Fig. 1a). The use of nonionic surfactants (*i.e.*, Tween 80 and Span 85) in water solution facilitated the emulsification and stabilization of the nanoemulsions, followed by the evaporation removal of chloroform. In particular, the presence of the ionized quaternary ammonium group in DOTAP not only facilitated the efficient embedding of MSA-2 *via* weak electrostatic interactions and van der Waals interactions, but also conferred

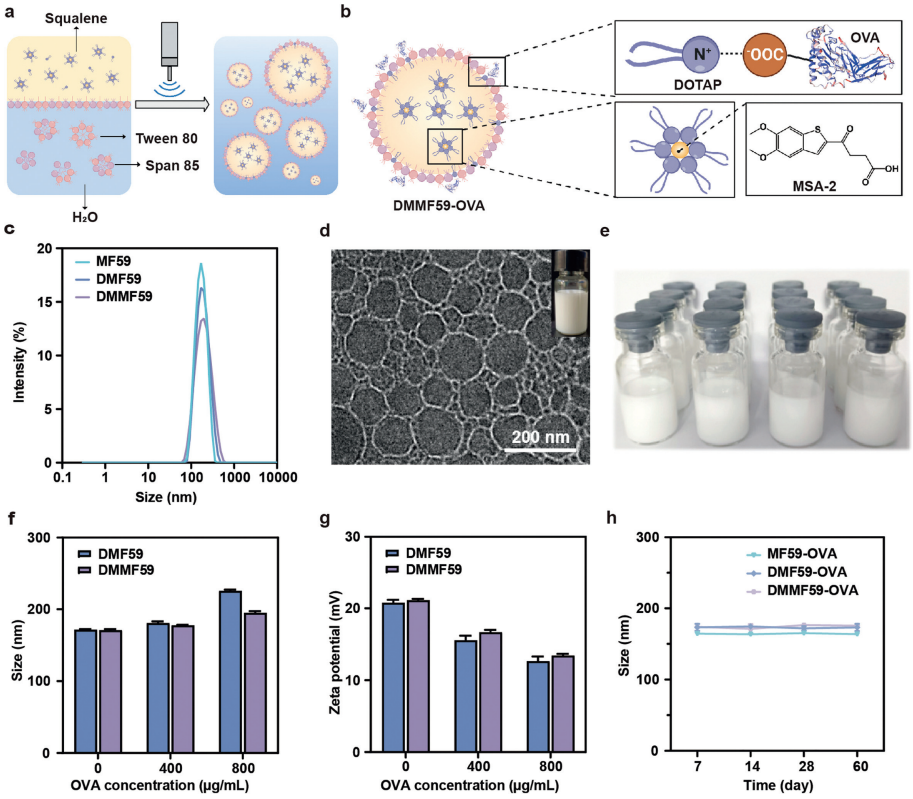


Fig. 1. (a) Nanoemulsions were prepared by ultrasonic emulsification from squalene, Tween 80, Span 85 and DOTAP, in this way emulsion achieved the loading of MSA-2 and OVA *via* the positive electrical groups of cationic lipids. (b) The schematic diagram of the construction of DMMF59-OVA. (c) The size distribution of MF59, DMF59 and DMMF59. (d) The cryo-TEM and digital image (inset) of DMMF59-OVA. (e) The appearance of nanovaccine. (f) Hydrodynamic diameter of DMF59 and DMMF59 under load with different concentration of OVA. (g) Zeta potential of DMF59 and DMMF59 under load with different concentration of OVA. (h) Particle size change of various formulations stored at 4 °C for 60 days. Data are presented as the mean ± SD ($n = 3$).

a positive charge to the emulsion surface, allowing the model antigen OVA to be adsorbed by electrostatic interactions to yield DMMF59-OVA or none MSA-2 loaded DMMF59-OVA (DMF59-OVA) (Fig. 1b) [49,50]. Dynamic light scattering (DLS) analysis revealed that the average particle sizes of MF59, DMF59 and DMMF59 were 163.9 ± 1.2, 170.2 ± 2.4 and 174.9 ± 0.9 nm, respectively, with all emulsion showed a narrow monodispersed unimodal size distribution pattern (0.11–0.16) (Fig. 1c and Table S1 in Supporting information). The morphology of DMMF59-OVA was observed by cryogenic transmission electron microscopy (cryo-TEM), revealing a spherical shape with an average size of approximately 140 nm (Fig. 1d). The nanovaccine of DMMF59-OVA can be produced in large scale *via* ultrasonic emulsification (Fig. 1e). Comparatively, the introduction of OVA increased the nanoemulsion size of the nanovaccine from ~170 nm to ~200 nm. Meanwhile, with the inclusion of OVA, the zeta potential decreased from ~20 mV to ~13 mV compared to the original cationic emulsion (Figs. 1f and g). Quantitative analysis revealed that the loading efficiency of MSA-2 and OVA was 96.3 % and 92.5 %, respectively. The high efficiency is attributed to the solubilizing effect of DOTAP on MSA-2 and the electrostatic interactions between DMMF59 and OVA. No obvious changes of the particle size and polydispersity index (PDI) were detected after 60 days' storage at 4 °C, indicating well stability of the formulations (Fig. 1h and Fig. S1 in Supporting information).

The cytotoxicity of the nanovaccine was assessed in DC2.4 and 3T3 cells using a methylthiazolyldiphenyl-tetrazolium bromide (MTT) assay. After incubating the cells with DMF59-OVA or DMMF59-OVA for 24 h, the results showed that even at a squalene concentration of up to 1000 μg/mL, the cell viability of both cell types remained above 90 %, indicating good cytocompatibility of the emulsion delivery system (Figs. S2 and S3 in Supporting information). To observe internalization of antigen by APCs, DC2.4 cells were incubated with free Cy5-OVA, MF59-Cy5-OVA, DMF59-Cy5-OVA or DMMF59-Cy5-OVA for 12 h. As shown in Fig. S4 (Supporting information), flow cytometry analysis revealed that OVA-positive cells in the DMF59-Cy5-OVA and DMMF59-Cy5-OVA groups were 88.83 % and 72.66 %, respectively, which were 2.94 and 2.40 times higher than the free Cy5-OVA group, while MF59-Cy5-OVA showed no significant effect on enhancing OVA uptake (Fig. S4a). The mean fluorescence intensity (MFI) of DMF59-Cy5-OVA group was appropriately 2 times higher than that of the free Cy5-OVA (Fig. S4b). Confocal laser scanning microscopy (CLSM) also confirmed the intracellular localization of OVA antigen, showing that after incubation with DMF59-Cy5-OVA or DMMF59-Cy5-OVA, more red fluorescence signal was concentrated inside the cells compared to the other groups, consistent with the results of flow cytometry analysis (Fig. S5 in Supporting information).These results indicated that both DMF59 and DMMF59 promoted the uptake of OVA compare to MF59 due to the strong interaction of the large amount of positive charges on cationic emulsion with lipids in the cell membrane [51]. The enhanced cellular uptake of antigen by APCs could potentially improve antigen cross-presentation and increase the efficacy of vaccination.

Since the activation of APCs performs a pivotal function in antigen presentation and the priming of adaptive immune responses, an investigation was conducted to ascertain the capacity of the nanovaccine to activate bone marrow-derived dendritic cell (BMDCs) [52]. The surface expression of CD80 and CD86 on DCs after co-cultivation with different formulations were assessed by flow cytometry (Fig. S6 in Supporting information). Compared to free OVA, MF59-OVA treatment resulted in only a modest increase in CD80 expression, whereas DMMF59-OVA significantly enhanced the expression of both CD80 and CD86. Specifically, DMMF59-OVA induced CD80 and CD86 expression levels that were 1.23 and 1.3 times higher, respectively, than those induced by DMF59-OVA. In addition to the up-regulation of costimulatory markers, BMDC

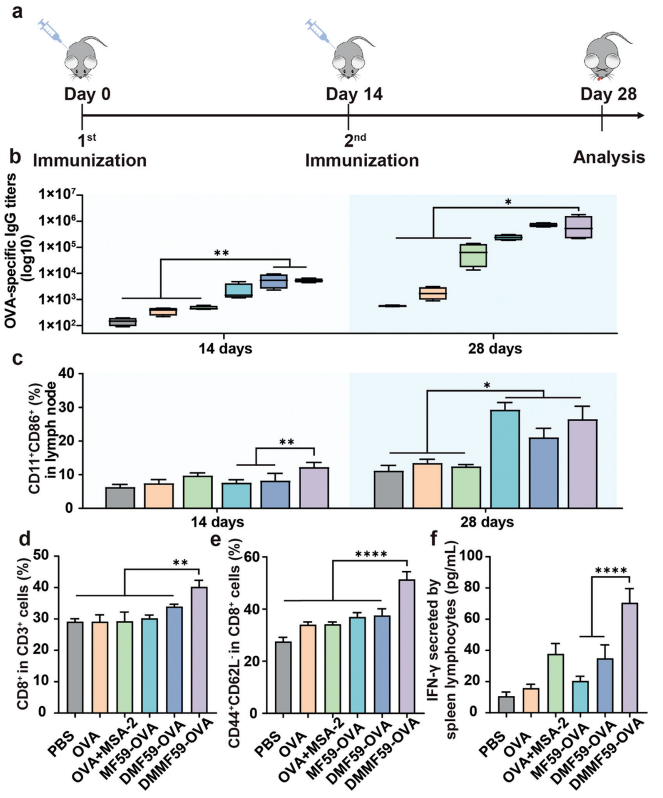


Fig. 2. (a) Schematic of immunization schedule. C57BL/6 mice were immunized on day 0, boosted on day 14, and the magnitude of the immune responses was evaluated on days 14 and 28. (b) OVA-specific IgG antibody levels on days 14 and 28 as detected by enzyme linked immunosorbent assay (ELISA). (c) The quantitative statistics of $CD11c^+CD86^+$ DC in lymph node on day 14 and day 28 by flow cytometry. The expression of CD8 on $CD3^+$ T cells (d) and CD44CD62L on $CD8^+$ T cells (e) in spleen were detected by flow cytometry. (f) IFN-γ-secreting splenocytes as detected by ELISA. Data are presented as the mean ± SD ($n = 4$). $^*P < 0.05$, $^{**}P < 0.01$, $^{****}P < 0.0001$.

maturation is associated with increased production of proinflammatory cytokines. Previous studies have demonstrated that MSA-2 activates the STING pathway by binding to its transmembrane domain, triggering conformational changes, which promote type I interferon production and pro-inflammatory cytokine responses (*e.g.,* IL-6, TNF-α) through downstream TBK1-IRF3 signaling. It was found that DMMF59-OVA treatment enabled effective secretion of IFN-β, indicating the activation of STING pathway, while secretion levels in cells treated with other formulations remained below 100 pg/mL (Fig. S7 in Supporting information). Moreover, BMDCs secreted the highest levels of IL-6, TNF-α and IFN-γ after incubation with DMMF59-OVA compared to other groups (Fig. S8 in Supporting information). Taken together, the results revealed that the DMMF59-OVA nanovaccine-mediated codelivery of antigen and STING agonists was crucial to promote the antigen uptake, APCs maturation and the STING pathway activation.

Based on the *in vitro* experiment results, the potential of the nanovaccine to induce antigen-specific immune responses *in vivo* was evaluated. All animal experiment procedures were approved by the Animal Ethics Committee of Shandong University (approval No. 22012). C57BL/6 mice were intramuscularly vaccinated with different formulations on day 0, boosted on day 14, and euthanized on day 28 (Fig. 2a). To validate the activation of the STING signaling pathway and its contribution to the antitumor immune response, cytokine levels of CXCL10, and TNF-α in the serum of immunized mice were examined. Compared to the DMF59-OVA group, the DMMF59-OVA group showed higher cytokine levels in the serum, confirming the significant role of MSA-2 in activating

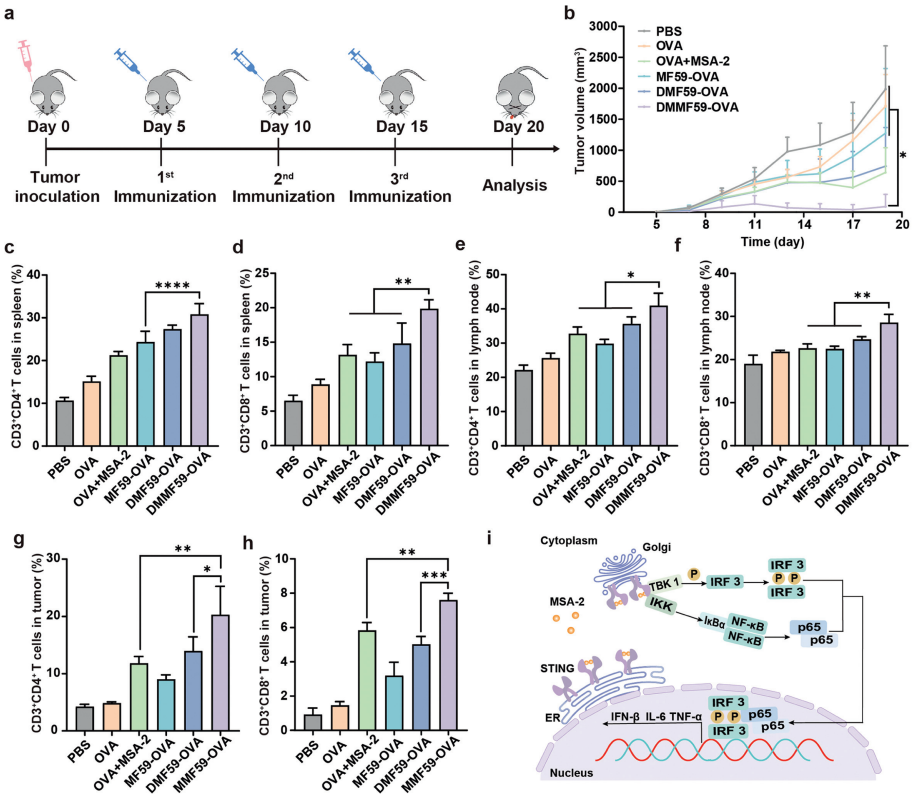


Fig. 3. (a) Tumor inoculation and immunization strategy. (b) Tumor volume changes during treatments. The amount of $CD3^+CD4^+$ T cells (c) and $CD3^+CD8^+$ T cells (d) in spleens. The amount of $CD3^+CD4^+$ T cells (e) and $CD3^+CD8^+$ T cells (f) in lymph nodes. The amount of $CD3^+CD4^+$ T cells (g) and $CD3^+CD8^+$ T cells (h) in tumors. (i) Schematic illustration of the mechanism of MSA-2 activating the STING pathway. Data are presented as the mean ± SD ($n = 6$). $^*P < 0.05$, $^{**}P < 0.01$, $^{***}P < 0.001$, $^{****}P < 0.0001$.

the STING pathway (Fig. S9 in Supporting information). To assess the immune response, OVA-specific antibody titers in the serum of immunized mice were measured. As shown in Fig. 2b, mice receiving nanovaccine-based formulations displayed elevated IgG titers by day 14. The difference became more pronounced after the booster injection, with the DMMF59-OVA formulation eliciting the highest antibody levels. The ability of the nanovaccine to activate lymph node-resident DCs was also examined. No significant difference was observed among the six individual groups after a single injection. However, after the second immunization, the $CD11c^+CD86^+$ populations were significantly higher in the MF59-OVA, DMF59-OVA, and DMMF59-OVA groups than in the others (Fig. 2c). On the same day, spleens of vaccinated mice were isolated and processed to obtain single splenocytes for flow analysis.

As shown in Fig. 2d, the DMMF59-OVA elevated the proportion of $CD8^+$ T cells. To investigate the ability of nanovaccine to elicit adaptive immune response, the obtained single splenocytes were restimulated with OVA antigen *in vitro*. Among all groups, the DMMF59-OVA group exhibited the highest number of effector memory T cells ($CD44^+CD62L^-$), and the secretion of IFN-γ stimulated by DMMF59-OVA was 1.87- and 2.02-fold higher than that of OVA+MSA-2 and DMF59-OVA, respectively (Figs. 2e and f). This phenomenon indicated that MF59-OVA could also induce certain levels of IgG owing to the superiority of traditional emulsion adjuvant, but its capacity to stimulate $CD8^+$ T cell responses was significantly insufficient. Simultaneously, the DMMF59-OVA dual adjuvant delivery system was found to be the most effective in achieving the highest level of antibody titers, and triggered stronger adaptive immune response and immune memory effect [53,54].

To confirm the antitumor effect of nanovaccine, the therapeutic effect and immune activation capabilities were assessed in the E.G7-OVA tumor model. C57BL/6 mice were subcutaneously injected with tumor cells in the right flank, and they were treated with various formulations on day 5, with a total of three immunizations (Fig. 3a). The results revealed that, in comparison with the PBS group, DMMF59-OVA substantially inhibited the tumor growth, while OVA+MSA-2 and DMF59-OVA immunization exhibited a moderate capacity to impede the progression of the tumor. Free OVA or MF59-OVA was not effective against tumor growth (Fig. 3b). Additionally, the tumor growth curves of each mouse further confirmed the antitumor effect of the nanovaccine. For instance, by day 17, mice in DMMF59-OVA group showed a tumor volume of below 200 mm^3, while that in DMF59-OVA group over 380 mm^3, and with 4 out of 6 mice in former group completely rejecting the tumor at the end of immunization (Fig. S10 in Supporting information). In addition, no obvious changes of body weight in all groups, suggesting minimal *in vivo* toxicity (Fig. S11 in Supporting information).

To explore the relationship of the therapeutic effect and systemic immune activation, the proportion of T cells in crucial secondary lymphoid organs (*i.e.*, spleen and lymph nodes) was analyzed, since DCs engage with T lymphocytes in order to elicit adaptive immune responses in these organs [55,56]. As shown in Figs. 3c and d, and Fig. S12 in Supporting information, the spleen of mice treated with DMMF59-OVA exhibited the highest frequency of $CD3^+CD4^+$ and $CD3^+CD8^+$ T cells, which were 1.27 and 1.63 times higher than that of MF59-OVA group, respectively. A similar trend was observed in T lymphocytes from lymph nodes (Figs. 3e and f). Then, we analyzed the tumor-infiltrating immune cells. As shown in Figs. 3g and h, the percentages of $CD3^+CD4^+$ and $CD3^+CD8^+$ T cells in DMMF59-OVA-treated group were 20.30 % and 7.60 % respectively, which were 1.72, 2.25, 1.45 times and 1.30, 2.38, 1.51 times that of OVA+MSA-2, MF59-OVA, and DMF59-OVA treated mice. Immunofluorescence staining of tumor

tissue sections further confirmed these results, showing heightened infiltration of $CD8^+$ and $CD4^+$ T cells in the DMMF59-OVA group compared to other groups (Fig. 3i).

In addition, effective activation of $CD8^+$ effector T cells (IFN-γ^+CD8^+ T cells) in the DMMF59-OVA than that of the PBS indicated the establishment of antigen-specific cellular immune responses (Fig. S13 in Supporting information). Terminal deoxynucleotidyl transferase mediated dUTP nick-end labeling (TUNEL)-staining analysis demonstrated that more cells in the tumor were apoptotic after DMMF59-OVA treatment (Fig. S14 in Supporting information). As a predominant Th2 adjuvant, MF59 can elicit potent humoral immunity but not cellular immunity, which accounted for the unsatisfactory antitumor effects of MF59-OVA and DMF59-OVA in our work. In contrast, the remarkable tumor inhibition effect of DMMF59-OVA might should benefit from the synergistic effect produced by the emulsion acting as both an adjuvant and a carrier co-delivering antigen and STING agonist MSA-2, therefore stimulated robust humoral and cellular immune responses (Fig. S15 in Supporting information) [57–59]. Additionally, immunofluorescence staining of natural killer (NK) cells in tumor slices was performed to assess their infiltration within the tumor microenvironment. The results confirmed the robust activation of the STING pathway and highlighted the involvement of NK cells in the tumor immune response, further supporting the role of STING activation in mediating specific antitumor immunity (Fig. S16 in Supporting information).

As shown in Fig. S17 (Supporting information), the immunization did not cause abnormal expression in lactic dehydrogenase (LDH), alanine aminotransferase (ALT), alkaline phosphatase (ALP) or urea (UREA), suggesting that DMMF59-OVA could not induce heart, liver or kidney damage, and the same result was reflected in the viscera indexes (Fig. S18 in Supporting information). Furthermore, hematoxylin-eosin (H&E) staining of major organs, including the heart, liver, spleen, lungs, and kidneys, revealed no obvious cell apoptosis or necrosis after treatment (Fig. S19 in Supporting information). These findings confirmed the well biocompatibility and low systemic toxicity of the nanovaccines employed in this study, making DMMF59-OVA a safe and promising candidate for clinical translation in cancer immunotherapy.

In summary, we developed a nanovaccine-based vaccine of DMMF59-OVA, which could co-deliver OVA and MSA-2. This delivery system facilitated efficient antigen internalization and activation of APCs through the STING pathway. The reported vaccine demonstrated its ability to induce robust antibody- and cell-based immune responses, resulting in significant tumor inhibition in a murine tumor model. The modified formula of emulsions effectively harnessed the benefits of traditional emulsions and potentially established a novel immune adjuvant platform. In the combination of well-tolerated excipients and a straightforward preparation process, DMMF59-OVA as a vaccine delivery system holds promise with potential for cancer immunotherapy.

Declaration of competing interest

The authors declare that they have no known competing financial interests or personal relationships that could have appeared to influence the work reported in this paper.

CRediT authorship contribution statement

Xue Ma: Writing – original draft, Methodology, Investigation, Formal analysis, Data curation. **Anning Li:** Writing – review & editing, Methodology, Formal analysis, Data curation, Conceptualization. **Zhiliang Gao:** Writing – review & editing, Supervision, Investigation, Funding acquisition, Conceptualization. **Ning Wang:** Validation, Project administration, Formal analysis, Data curation, Conceptualization. **Mengqi Li:** Writing – review & editing, Investigation, Formal analysis. **Kanaparedu P.C. Sekhar:** Validation, Supervision, Methodology. **Muthupandian Ashokkumar:** Writing – review & editing, Methodology, Conceptualization. **Shumei Zhai:** Project administration, Data curation, Conceptualization. **Jiwei Cui:** Writing – review & editing, Supervision, Funding acquisition. **Qun Yu:** Writing – review & editing, Supervision, Project administration, Funding acquisition.

Acknowledgments

This work was financially supported by the National Natural Science Foundation of China (No. 22202117), the Foundation for Innovation Improvement of Science and Technology-Based Enterprises of Shandong Province (No. 2022TSGC1079), the International Cooperation Project of Shandong Province (No. WST2021019), and the Center for International Cooperation and Disciplinary Innovation (No. B20033). This work was performed in part at the Analytical Centre for Structural Constituent and Physical Property at Shandong University.

Supplementary materials

Supplementary material associated with this article can be found, in the online version, at doi:10.1016/j.cclet.2025.111410.

References

[1] D.S. Chen, I. Mellman, Immunity 39 (2013) 1–10.
[2] P. Sharma, J.P. Allison, Science 348 (2015) 56–61.
[3] S. Depil, P. Duchateau, S.A. Grupp, G. Mufti, L. Poirot, Nat. Rev. Drug Discov. 19 (2020) 185–199.
[4] J. Liu, M. Fu, M. Wang, et al., J. Hematol. Oncol. 15 (2022) 28.
[5] T. Nie, Y. Fang, R. Zhang, et al., Bioact. Mater. 47 (2025) 51–63.
[6] S. Han, Z. Zhao, J. Wu, Mil. Med. Res. 11 (2024) 12.
[7] D.S. Chen, I. Mellman, Nature 541 (2017) 321–330.
[8] T.L. Whiteside, S. Demaria, M.E. Rodriguez-Ruiz, H.M. Zarour, I. Melero, Clin. Cancer Res. 22 (2016) 1845–1855.
[9] T. Nie, H. Liu, Z. Fang, et al., ACS Nano 17 (2023) 10925–10937.
[10] S. Han, J. Wu, Bioact. Mater. 17 (2022) 300–319.
[11] B. Pulendran, P.S. Arunachalam, D.T. O'Hagan, Nat. Rev. Drug Discov. 20 (2021) 454–475.
[12] Y. Li, Z. Chen, X. Lu, et al., Nano Res. 16 (2023) 13322–13334.
[13] Z. Hu, P.A. Ott, C.J. Wu, Nat. Rev. Immunol. 18 (2017) 168–182.
[14] G. Shang, C. Zhang, Z.J. Chen, X. Bai, X. Zhang, Nature 567 (2019) 389–393.
[15] P. Gao, M. Ascano, Y. Wu, et al., Cell 153 (2013) 1094–1107.
[16] X. Zhang, H. Shi, J. Wu, et al., Mol. Cell 51 (2013) 226–235.
[17] H. Ishikawa, G.N. Barber, Nature 455 (2008) 674–678.
[18] J. Zheng, J. Mo, T. Zhu, et al., Mol. Cancer 19 (2020) 133.
[19] Y. He, C. Hong, S. Huang, et al., Adv. Healthc. Mater. 12 (2023) 2300688.
[20] Z. Gao, N. Wang, Y. Ma, et al., Nano Today 54 (2024) 102096.
[21] D. Wang, T. Nie, C. Huang, et al., Small 18 (2022) 2203227.
[22] Y. Cai, Y. Jiang, Y. Chen, et al., Chin. Chem. Lett. 36 (2025) 110437.
[23] S. Liang, J. Yao, D. Liu, et al., Chin. Chem. Lett. 36 (2025) 109856.
[24] S. Yum, M. Li, A.E. Frankel, Z.J. Chen, Annu. Rev. Cancer Biol. 3 (2019) 323–344.
[25] G. Berger, M. Marloye, S.E. Lawler, Trend. Mol. Med. 25 (2019) 412–427.
[26] W. Sun, H. Wang, Y. Qi, et al., ACS Nano 18 (2024) 23727–23740.
[27] C. Li, Y. Zhang, Y. Wan, et al., Chin. Chem. Lett. 32 (2021) 1615–1625.
[28] L. Deng, H. Liang, M. Xu, et al., Immunity 41 (2014) 843–852.
[29] J.M. Ramanjulu, G.S. Pesiridis, J. Yang, et al., Nature 564 (2018) 439–443.
[30] T.F. Gajewski, E.F. Higgs, et al., Science 369 (2020) 993–999.
[31] J. Yu, S. He, C. Zhang, et al., Angew. Chem. Int. Ed. 62 (2023) e202307272.
[32] C. Ding, M. Du, Z. Xiong, et al., Chem. Sci. 14 (2023) 5956–5964.
[33] X. Chen, F. Meng, Y. Xu, et al., Nat. Commun. 14 (2023) 4584.
[34] Y. Li, R. Zhu, Y. Guo, et al., Chin. Chem. Lett. 35 (2024) 110704.
[35] F. Chen, T. Li, H. Zhang, et al., Adv. Mater. 35 (2023) 202209910.
[36] J. Jiang, M. Zhang, T. Lyu, et al., Adv. Mater. 35 (2023) 2300854.
[37] B.S. Pan, S.A. Perera, J.A. Piesvaux, et al., Science 369 (2020) eaba6098.
[38] F. Mosca, E. Tritto, A. Muzzi, et al., Proc. Natl. Acad. Sci. U. S. A. 105 (2008) 10501–10506.
[39] C.B. Fox, L. Barnes V, T. Evers, et al., Viruses 7 (2012) 815–826.
[40] K. Hormann, A. Zimmer, J. Control. Release 223 (2016) 85–98.
[41] D.T. O'Hagan, R. van der Most, R.N. Lodaya, M. Coccia, G. Lofano, npj Vaccines 6 (2021) 158.
[42] C. Ye, J. Zhang, J. Shen, et al., Chin. Chem. Lett. 35 (2024) 110519.
[43] A. Seubert, S. Calabro, L. Santini, et al., Proc. Natl. Acad. Sci. U. S. A. 108 (2011) 11169–11174.

[44] D.T. O'Hagan, G.S. Ott, G.V. Nest, R. Rappuoli, G.D. Giudice, Expert Rev. Vaccine. 12 (2014) 13–30.
[45] M. Vono, M. Taccone, P. Caccin, et al., Proc. Natl. Acad. Sci. U. S. A. 110 (2013) 21095–21100.
[46] S. Shi, H. Zhu, X. Xia, et al., Vaccine 37 (2019) 3167–3178.
[47] M.F. Bachmann, G.T. Jennings, Nat. Rev. Immunol. 10 (2010) 787–796.
[48] D.T. O'Hagan, G.S. Ott, E. De Gregorio, A. Seubert, Vaccine 30 (2012) 4341–4348.
[49] S.Y. Kim, S. Kim, J.E. Kim, et al., ACS Nano 13 (2019) 12671–12686.
[50] A. Taha, E. Ahmed, A. Ismaiel, et al., Trends Food Sci. Technol. 105 (2020) 363–377.
[51] H. Jiang, Q. Wang, L. Li, et al., Adv. Sci. 5 (2017) 1700426.
[52] R.M. Steinman, Nat. Med. 13 (2007) 1155–1159.
[53] A.K. Blakney, P.F. McKay, D. Christensen, et al., J. Control. Release 304 (2019) 65–74.
[54] Z. Chen, X. Hao, H. Wang, J. Control. Release 349 (2022) 699–711.
[55] S.M. Lewis, A. Williams, S.C. Eisenbarth, Sci. Immunol. 4 (2019) eaau6085.
[56] A. Schudel, D.M. Francis, S.N. Thomas, Nat. Rev. Mater. 4 (2019) 415–428.
[57] H.H. Tayeb, R. Felimban, S. Almaghrabi, N. Hasaballah, Colloid Interface Sci. Commun. 45 (2021) 100533.
[58] Y. Shi, Y. Lu, B. Qin, et al., Nano Today 41 (2021) 101326.
[59] Y. Tahara, R. Mizuno, T. Nishimura, et al., Biomaterials 282 (2022) 121385.